Pergamon

Bioorganic & Medicinal Chemistry 8 (2000) 329–335

BIOORGANIC & MEDICINAL CHEMISTRY

Density Functional and Ab Initio Studies on *N*-Acetyl-Duocarmycin SA: Insight Into Its DNA Interaction Properties

Karl N. Kirschner,[a] Moses Lee,[b] Robert C. Stanley[b] and J. Phillip Bowen[a,*]

[a]*Computational Center for Molecular Structure and Design, Department of Chemistry, University of Georgia, Athens, GA 30602-2556, USA*

[b]*Department of Chemistry, Furman University, Greenville, SC 29613, USA*

Received 18 June 1999; accepted 22 September 1999

Abstract—Density functional (DF) and Møller-Plesset second order perturbation (MP2) calculations were carried out on *N*-acetyl-duocarmycin SA (*N*-Ac-DSA), an analogue of a series of potent antitumor antibiotics that include the duocarmycins. These computational methods were used to investigate the degree of ground state destabilization of duocarmycins that would result upon binding to DNA. Ground state destabilization has been proposed as the origin of the ligand's enhanced rate of alkylation by more than a millionfold. The conformations of the '**Unbound**' and 'DNA-**Bound**' *N*-Ac-DSA were generated using available geometric data for duocarmycin SA. Specifically, the dihedral angles $\chi 1/\chi 2$ were locked at 6.9°/4.5° for the **Unbound** and 22.0°/11.0° for the **Bound** form. The structures were optimized using DF theory, with subsequent MP2 calculations to improve the electronic energies. All of the calculations were performed on the unprotonated (**1**) as well as the C6-carbonyl protonated form (**2**). The results showed that the ground state destabilization energies of the **Unbound** and **Bound** forms, for the unprotonated and protonated series, were fairly small (< 0.8 kcal/mol). Similarly, the difference in the electronic nature of the **Unbound** and **Bound** forms, as indicated by changes in bond lengths and charge density, were also small. In summary, it appears that twisting of two key torsional angles, the concomitant ground state destabilization, and C6-carbonyl protonation may not fully account for the significant rate increase of adenine-N3 alkylation upon binding to DNA.

Introduction

In recent years there has been an interest in structurally similar potent antitumor antibiotics because of their ability of sequence selective recognition and alkylation of DNA.[1–6] These ligands include (+)-CC-1065,[7] (+)-duocarmycin SA,[8] and (+)-duocarmycin-A,[9,10] all of which bind selectively to AT-rich sites in DNA's minor groove and appear to have significantly enhanced rate of adenine-N3 alkylation upon binding to DNA.[2–6] The common structural characteristics of these ligands are a reactive cyclopropyl ring, an indole ring, and significant double bond conjugation involving several rings and heteroatoms. Elucidation of why these molecules have such high sequence selective recognition and have been characterized as 'catalytic' in nature has given way to two different hypotheses: (1) alkylation site model[5,6] and (2) noncovalent binding model.[11–13] Both hypotheses are based on the structure–activity relationship paradigm.

The alkylation site model suggests that the DNA sequence which is most capable of adopting the 'active' conformation at the least cost of internal energy will preferentially react with these ligands.[5,6] The structural changes in DNA will bring the reactive nucleophilic atom (adenine-N3) into covalent bonding range for reaction with the cyclopropyl ring of these ligands. The rate of reaction is then increased by protonation of the C6-carbonyl.[5,14] Another important feature for rate enhancement, according to this hypothesis, is the size of the side chain attached to the 'active' portion of the molecule. The longer side chains increase the ligand–DNA interactions which in turn increase the reaction rate constant for adduct formation.[6]

The noncovalent binding model states that ground state destabilization of these ligands causes the enhancement in rate of DNA alkylation.[11–13] A prerequisite for this model is the electrostatic and hydrogen bonding

Keywords: duocarmycin; molecular modeling; ground state destabilization; antitumor compound.

*Corresponding author. Tel.: +1-706-542-2626; fax: +1-706-542-9454.

0968-0896/00/$ - see front matter
PII: S0968-0896(99)00278-3

interactions between the ligand and the specific DNA base pairs which govern the sequence selectivity recognition.[15–18] These ligands bind specifically in the minor groove because of enhanced van der Waals contacts present in the sterically deeper AT-rich sites over GC-rich sites or the wider major groove region.[1,4,18] Coinciding with specificity is the high affinity of these ligands for AT-rich sites. This is also due to favorable electrostatic and hydrogen bonding interactions between the ligand and DNA.[15] Upon recognition, twisting of key torsion angles within the ligand causes two different types of electron delocalization disruption.[12,13] Twisting of one torsion angle diminishes the conjugation between the N^2 vinylogous amide and the cyclohexadienone, which in turn may activate the cyclopropyl ring for nucleophilic attack. Alternatively, twisting of a second torsion angle disrupts the amide resonance, enhancing the N^2 vinylogous amide conjugation leading to easier C6-carbonyl protonation or enhancement of metal cation complexation. These induced conformational changes are a result of the ligand adopting the curvature and pitch of the minor groove.[13,16]

In this study, density functional (DF) and ab initio theory were used to determine the degree of ground state destabilization of the ligand along with examination of structural and electronic changes that could cause the enhanced rate of DNA alkylation. This was done by comparing relative electronic energies, geometric parameters, partial charge distributions, highest occupied molecular orbital (HOMO) energy, and lowest unoccupied molecular orbital (LUMO) energy of *N*-Ac-DSA as functions of the two important torsional angles suggested to be involved in the mechanism of action.[12,13] Due to the size of (+)-CC-1065, (+)-duocarmycin SA, and (+)-duocarmycin A and their high computational cost, we decided to investigate *N*-Ac-DSA, a smaller analogue (Fig. 1) which contains all of the important structural characteristics.[4,5,12,13,19] This analogue is less efficient at alkylating DNA due to the small size of the right hand subunit since it does not induce enough of a twist in the amide that a larger subunit is suggested to provide.[11] This was overcome by freezing the geometries such that a significant twist exists (see Experimental and Results). Results from the investigation of this analogue should be applicable to the larger duocarmycins and (+)-CC-1065.

Results and Discussion

The torsion angles $\chi1$ and $\chi2$ were selected for investigation based on experimental and theoretical results. The X-ray structure of *N*-BOC-DSA was used to obtain the torsion angles $\chi1 = 6.9°$ and $\chi2 = 4.5°$, and are assumed to correspond closely to the unbound solution phase conformation (**1**-, **2-Unbound**).[3,13] High field NMR studies and restrained molecular dynamics calculations on DSA bound in the minor groove (of dGACTAATTGAC.dGTCATTAGTC) revealed a bound conformation possessing torsion angles $\chi1 = 22°$ and $\chi2 = 11°$ (**1**-, **2-Bound**).[13,25,26] Our fully optimized structures (without torsional constraints) correspond to the gas phase conformations which are not influenced by any molecular environment (i.e. solvent or DNA) (**1**-, **2-GP**). Table 1 reports the relative energies between the **Unbound**, **Bound** and **GP** conformations for **1** and **2**. B3LYP results suggest that $\sim +0.42$ kcal/mol of internal energy is required as the conformation changes from **1-Unbound** to **1-Bound**. Increasing the level of theory to MP2 and the orbital space about the analogue reduces the relative energy to $\sim +0.27$ kcal/mol. If the assumption is made that the difference in energy between the two conformations is due to the decreased delocalization of electrons, then these results suggest that twisting of $\chi1$ and $\chi2$ does not significantly effect the electronic nature of the analogue. Following the noncovalent binding model, if electron delocalization is not disrupted and ground state destabilization is small, then the cyclopropyl ring might not be fully activated for nucleophilic attack, suggesting that ground state destabilization may not be the only source for DNA alkylation rate enhancement. Interestingly, if the analogue is protonated at the C6-carbonyl the relative energies between the **2-Unbound** and **2-Bound** increase at both levels of theory ($\sim +0.98$ kcal/mol for B3LYP and $\sim +0.76$ kcal/mol for MP2). The protonated species appears to be influenced more by changes in the torsion angles than the neutral species, but these relative energetic differences cannot fully account for the significant rate enhancement.

The gas-phase structure of the **Unbound** and **Bound** lie very close together on the potential energy surface for both **1** and **2** in terms of geometries and energetics. This suggests that the local potential energy surface, which describes the changes in the torsion angles, is relatively

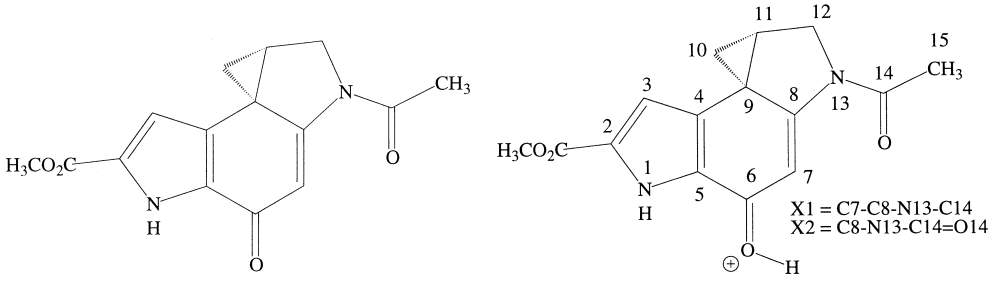

N-Ac-DSA, **1** Protonated *N*-Ac-DSA, **2**

Figure 1. Structures and the numbering system for *N*-acetyl-duocarmycin SA, **1**, and its C6-carbonyl protonated form, **2**.

Table 1. Results for **12-GP**, **1**, **2-Unbound** and **1**, **2-Bound** (dipole moments are in debye and energies are in kcal/mol)

	χ1	χ2	B3LYP dipole (MP2)[a]	B3LYP HOMO (MP2)	B3LYP LUMO (MP2)	B3LYP relative energy	MP2 relative energy
1-(Neutral)							
Basis functions						343	469
Gas Phase	13.1°	4.5°	8.661 (10.298)	−5.195 (−7.329)	−1.426 (1.069)	0.000[b]	0.000[c]
Unbound	6.9°	4.5°	8.683 (10.327)	−5.189 (−7.323)	−1.418 (1.064)	0.100	0.108
Bound	22.0°	11.0°	8.549 (10.156)	−5.204 (−7.341)	−1.446 (1.082)	0.515	0.381
2-(Protonated)							
Basis functions						345	474
Gas Phase	9.1°	3.3°	4.615 (5.731)	−8.351 (−10.278)	−5.260 (−2.586)	0.000[d]	0.000[e]
Unbound	6.9°	4.5°	4.617 (5.731)	−8.350 (−10.277)	−5.258 (−2.585)	0.015	0.000
Bound	22.0°	11.0°	4.553 (5.648)	−8.346 (−10.279)	−5.275 (−2.596)	0.999	0.761

[a]CHELPG dipole.
[b]−990.4218917 hartree.
[c]−987.6415441 hartree.
[d]−990.8083982 hartree.
[e]−988.0177476 hartree.

flat. A potential source for error in these results is neglection of solvent or DNA's minor groove. The solvent and/or DNA environment could change the geometries of **1**, **2-GP** and their relative stabilities compared to **1**, **2-Unbound** and **1**, **2-Bound** conformations since our calculations were done without considering the molecular environment specifically. Moreover, when the solvent/DNA environment is considered, one needs to consider free energies not just electronic energies as was done in this study. Because we are interested in the internal electron redistribution and its effect on relative stability, the comparison of electronic energies is justifiable in this study. Inclusion of solvent or DNA probably would not substantially change the conclusions of our calculations.

In addition to electronic energies, the molecular geometries, partial charges, HOMO and LUMO differences were examined for evidence of disruption of electron delocalization. Figure 2 displays B3LYP bond lengths for **1-GP**, **1-Unbound** and **1-Bound**. It has been suggested that subtle binding-induced changes in the ligand structure can result in large changes in reactivity.[13] Twisting of χ1 increases the amide conjugation which can result in an increase in the cyclopropyl ring reactivity. Twisting of χ2 diminishes the amide conjugation while increasing the N^2 vinylogous amide conjugation, thus increasing the basicity of the C6-carbonyl making protonation easier.[12,13] If twisting χ1 breaks the N^2 vinylogous amide delocalization, an increase in the C8–N13 bond length should be observed. Alternatively, twisting χ2 disrupts amide conjugation, then a lengthening of the N13-C14 bond should result. Neither is seen for the **GP**, **Unbound**, nor **Bound** conformations of *N*-Ac-DSA. The overall differences between the three geometries are minor, with the exception of χ1 and χ2, as seen in the results of an RMS analysis of the bond lengths, angles, and torsion angles (Table 2). Similar results are also seen for the protonated *N*-Ac-DSA (Fig. 3, Table 2).

If the twisting of these torsion angles alter the electron delocalization then a significant change in the partial charge distribution should occur. If altering the delocalization 'activates' the cyclopropyl ring, then a change in the partial charges within the ring should be

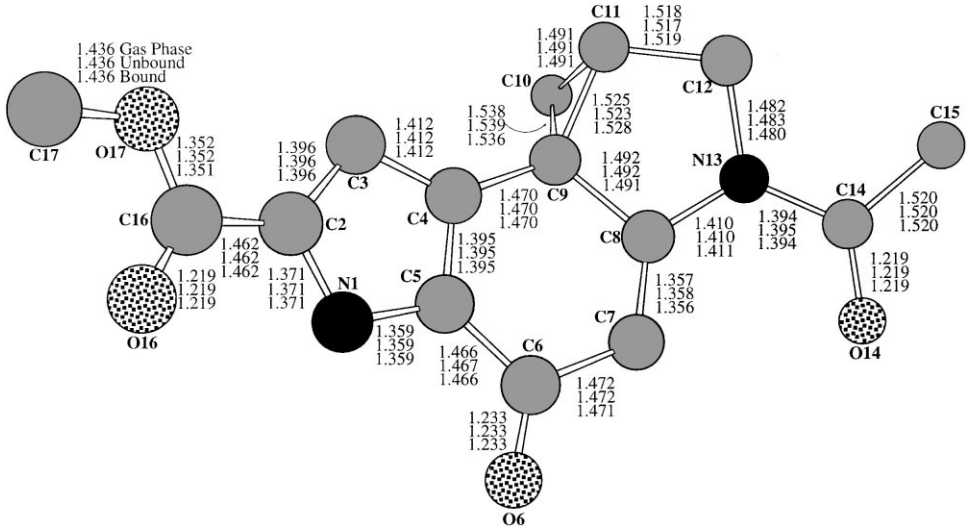

Figure 2. Bond lengths, in angstroms, of neutral *N*-Ac-DSA for the **Gas Phase**, **Unbound** and **Bound** conformations.

Table 2. RMS calculations between the **Unbound** and **Bound** conformations of **1** and **2** (only heavy atoms were used in calculating the RMS)

	RMS between **1-Unbound** and **1-Bound**	RMS between **2-Unbound** and **2-Bound**
Atomic position	0.132 Å	0.124 Å
Bond lengths	0.002 Å	0.002 Å
Bond angle	0.4°	0.3°
Out-of-plane angle	0.9°	0.1°
Torsional angle	4.5°	4.5°

calculated. Analysis reveals virtually no charge rearrangement (Figs 4 and 5) as $\chi 1$ and $\chi 2$ torsion angles change for **1** and **2**. Hence, it appears there is little change in the electron delocalization between the **GP**, **Unbound** and **Bound** conformations and, therefore, little activation of the cyclopropyl ring.

If electron delocalization was disrupted then evidence of this should also be seen in the orbital energies and shape. Examining the HOMO and LUMO energies reveals an insignificant change in their absolute values as a function of $\chi 1$ and $\chi 2$ for **1** or **2** (Table 1).* Rotation

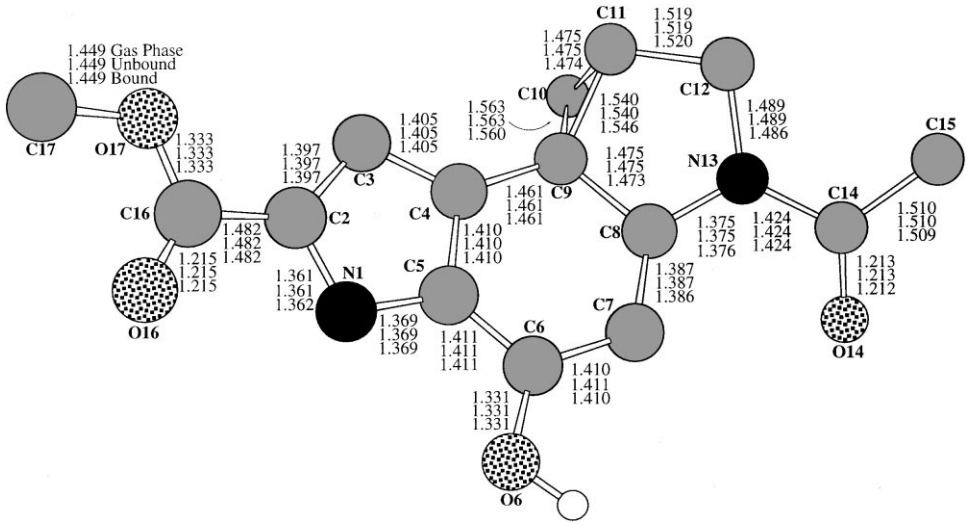

Figure 3. Bond lengths, in angstroms, of protonated *N*-Ac-DSA for the **Gas Phase**, **Unbound** and **Bound** conformations.

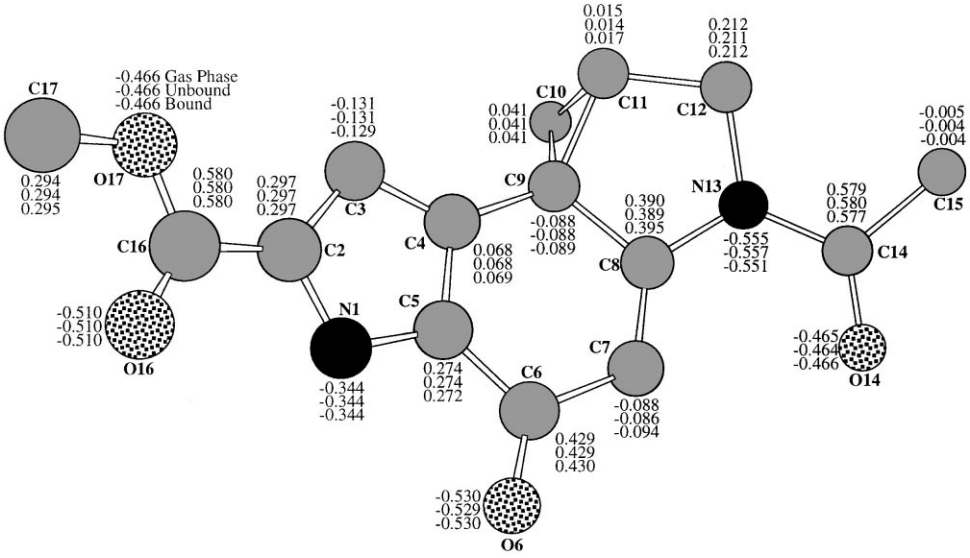

Figure 4. Mulliken atomic charges of neutral *N*-Ac-DSA for the **Gas Phase**, **Unbound** and **Bound** conformations. Hydrogen charges summed into heavy atoms.

*The experimental accuracy of the absolute HOMO and LUMO values calculated by DFT is questionable, as a referee commented. However, it is known that theory can be in absolute error to experimental properties (i.e. orbital energies) but relative comparisons between conformations result in a fortuitous cancellation of errors allowing for valid comparisons. A recent article[28] addresses the validity of DFT's absolute orbital energies and their qualitative shapes. The orbital shapes appear to be in agreement to other well established methods. Here we only use orbital energies to show that twisting of the torsions does not perturb the orbital energies.

about $\chi 1$ and $\chi 2$ does not significantly alter the location or shape of these orbitals for either **1** or **2**.[27] All of these results are consistent with the conclusion that as the analogue adopts its bound conformation from that in solution, there is not a significant change in the electronic nature of the molecule.

The only remarkable differences can be seen in comparing **1** to **2**. The bond length changes upon protonation are of the magnitude which is suggested to account for ligand activation due to ground state destabilization (a maximum being the carbonyl C6–O6 bond of 0.1 Å).[13] If very subtle changes in the ligand's geometry can account for rate enhancement, it lends support that protonation could also activate the ligand. The addition of the proton to the C6-carbonyl oxygen affects the N^2 vinylogous amide conjugation. Inspection of the partial charges reveal a slight change in the electronic nature of the molecule (Figs 4 and 5) which is also indicated by the change in bond lengths between **1** and **2** (Figs 2 and 3). The change in bond order can be represented in valence-bond terms by the simple shifting of double bonds (Fig. 6), which parallel the direction of change in bond lengths. Changes in partial charges, however, do not parallel this simple explanation. For example, based on the shifting of the double bonds and lone electron pair of N13, in a valence-bond argument, the nitrogen would become more positively charged; but based on the Mulliken partial charges, the nitrogen actually becomes more negative. It appears that the partial charges are redistributed throughout the molecule, thus making it more difficult to explain. However, based just on bond lengths, protonation appears to increase the N^2 vinylogous conjugation (shortening the C8–N13 and C6–C7 bond lengths, lengthening the C7–C8 and C6–O6 bond lengths) and decrease the amide conjugation (lengthening the C14–N13 bond length) which has been suggested to correspond to increase reactivity.[13]

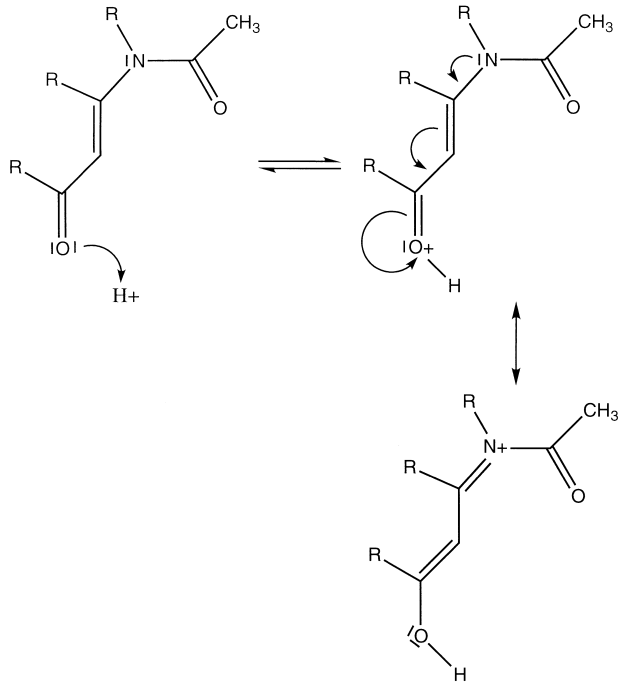

Figure 6. Valence bond argument showing the shifting double bonds in *N*-Ac-DSA upon protonation of the C6-carbonyl group.

The most dramatic change can be seen in the overall dipole, the protonated species is almost half the value (~4.6) of the neutral species (~8.7). Figure 7 depicts the dipole vector for the neutral and protonated species in the gas phase geometry. Upon protonation the dipole vector changes its orientation in space by ~40°. The positive end is directed inwards, towards the minor groove of DNA, while the negative end points out of the minor groove. However, the results for the magnitude and direction of the dipole moment for charged species is questionable. Recent investigations of the description of dipoles arising in charged species is being pursued.

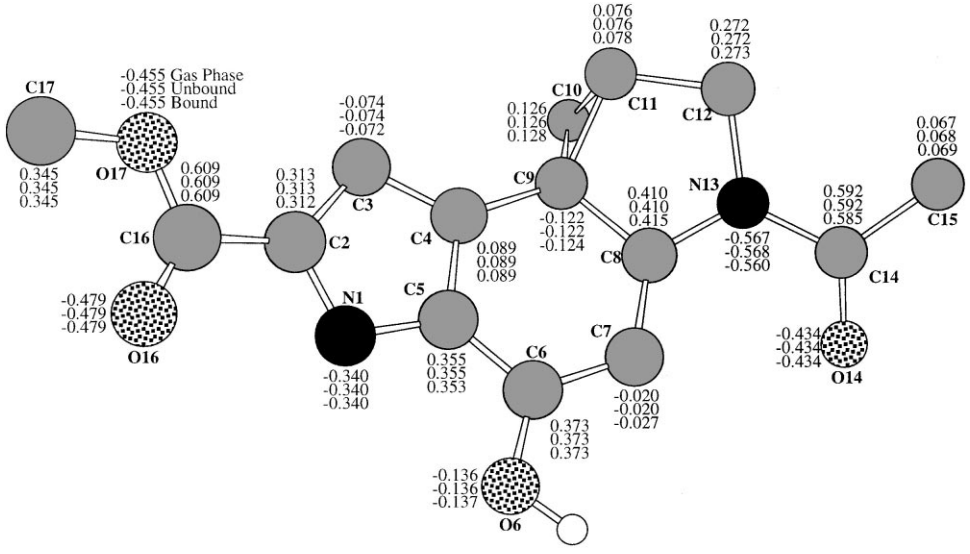

Figure 5. Mulliken atomic charges of protonated *N*-Ac-DSA for the **Gas Phase**, **Unbound** and **Bound** conformations. Hydrogen charges summed into heavy atoms.

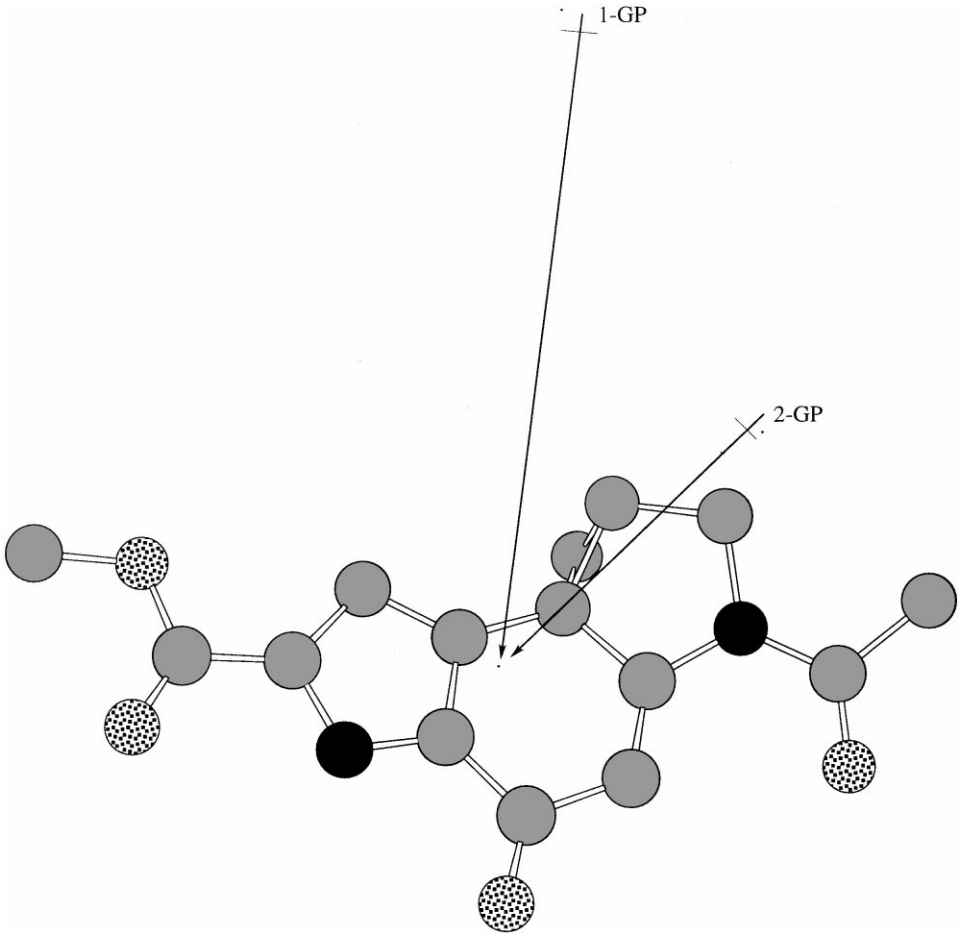

Figure 7. CHELPG graphical display of the relative magnitude and direction of the dipoles for neutral (**1-GP**) and protonated (**2-GP**) *N*-Ac-DSA.

Conclusion

Density functional and ab initio theories were used to investigate the degree of ground state destabilization of the neutral and protonated *N*-Ac-DSA, an analogue of the duocarmycins, that would result upon binding to DNA. Relative electronic, HOMO, and LUMO energies as well as bond lengths and partial charges were examined as a function of two important torsion angles for evidence of ground state destabilization. It appears that twisting of these torsional angles, the concomitant ground state destabilization, and C6-carbonyl protonation may not fully account for the significant rate increase of adenine-N3 alkylation upon binding to DNA.

Experimental

All calculations on the neutral (**1**; Fig. 1) and protonated *N*-Ac-DSA (**2**; Fig. 1) were carried out using the Gaussian94[20] program on a Silicon Graphics Origin 2000 cluster. Fully optimized structures were obtained using the density functional Becke Three Lee-Yang-Parr (B3LYP)[21] level of theory. These two structures are assumed to be minima since frequency calculations were too costly at this level of theory. Geometric constraints were applied to torsion angles $\chi 1$ (C7–C8–N13–C14) and $\chi 2$ (C8–N13–C14=O14) (Fig. 1, Table 1), and partial geometry optimizations followed. Single point calculations at the MP2 level of theory were performed on all B3LYP optimized structures to obtain improved electronic energies. Two different Pople basis sets were used in these calculations; the B3LYP calculations used 6-31G(d) and the MP2 calculations used 6-31 + G(d,p). The latter basis set includes the addition of diffuse functions on heavy atoms and polarization functions on hydrogens to describe better the orbital space around the molecule. The resulting number of basis functions implemented is reported in Table 1. Partial charges and dipoles were computed using the Mulliken[22,23] and CHELPG[24] formalisms. The graphics of the HOMO and LUMO were generated using the additional input commands CUBE = ORBITALS, HOMO, LUMO, and DENSITY.

Acknowledgements

We would like to thank the University Computing and Networking Services for providing resources for this investigation. This work was supported in part by the NSF-REU.

References and Notes

1. Dickerson, R. E.; Kopka, M. L.; Pjura P. E. In *DNA–Ligand Interactions From Drugs to Proteins*; Guschlbauer, W.; Saenger W., Eds.; Plenum Publishing: New York, 1987; pp 45–62.
2. Boger, D. L.; Boyce, C. W.; Johnson, D. S. *Bioorg. Med. Chem. Lett*. **1997**, *7*, 233.
3. Boger, D. L.; Goldberg, J.; McKie, J. A. *Bioorg. Med. Chem. Lett*. **1996**, *6*, 1955.
4. Boger, D. L.; Johnson, D. S. *Angew Chem., Int. Ed. Engl*. **1996**, *351*, 1438.
5. Hurley, L. H.; Warpehoski, M. A.; Lee, C.-S.; McGovren, J. P.; Scahill, T. A.; Kelly, R. C.; Mitchell, M. A.; Wicnienski, N. A.; Gebhard, I.; Johnson, P. D.; Bradford, V. S. *J. Am. Chem. Soc*. **1990**, *112*, 4633.
6. Hurley, L. H.; Lee, C.-S.; McGovren, J. P.; Warpehoski, M. A.; Mitchell, M. A.; Kelly, R. C.; Aristoff, P. A. *Biochem*. **1988**, *27*, 3886.
7. Chidester, C. G.; Krueger, W. C.; Mizsak, S. A.; Duchamp, D. J.; Martin, D. G. *J. Am. Chem. Soc*. **1981**, *103*, 7629.
8. Ichimura, M.; Ogawa, T.; Takahashi, K.; Kawamoto, E.; Yasuzawa, T.; Takahashi, I.; Nakano, H. *J. Antibiot*. **1990**, *43*, 1037.
9. Takahashi, I.; Takahashi, K.; Ichimura, M.; Morimoto, M.; Asano, K.; Kawamoto, I.; Tomita, F.; Nakano, H. *J. Antibiot*. **1988**, *41*, 1915.
10. Yasuzawa, T.; Muroi, K.; Ichimura, M.; Takahashi, I.; Ogawa, T.; Takahashi, K.; Sano, H.; Saitoh, S. H. *Chem. Pharm. Bull*. **1995**, *43*, 378.
11. Boger, D. L.; Bollinger, B.; Hertzog, D. L.; Johnson, D. S.; Cai, H.; Mesini, P.; Garbaccio, R. M.; Jin, Q.; Kitos, P. A. *J. Am. Chem. Soc*. **1997**, *119*, 4987.
12. Boger, D. L.; Garbaccio, R. M. *Bioorg. Med. Chem*. **1997**, *5*, 263.
13. Boger, D. L.; Hetzog, D. L.; Bollinger, B.; Johnson, D. S.; Cai, H.; Goldberg, J.; Turnbull, P. *J. Am. Chem. Soc*. **1997**, *119*, 4977.
14. Lin, C. H.; Beale, J. M.; Hurley, L. H. *Biochem*. **1991**, *30*, 3597.
15. Boger, D. L.; Invergo, B. J.; Coleman, R. S.; Zarrinmayeh, H.; Kitos, P. A.; Thompson, S. C.; Leong, T.; McLaughlin, L. W. *Chem.-Biol. Interact*. **1990**, *73*, 29.
16. Boger, D. L.; Sakya, S. M. *J. Org. Chem*. **1992**, *57*, 1277.
17. Boger, D. L.; Zhou, J.; Cai, H. *Bioorg. Med. Chem*. **1996**, *4*, 859.
18. Boger, D. L.; Munk, S. A.; Zarrinmayeh, H. *J. Am. Chem. Soc*. **1991**, *113*, 3980.
19. Boger, D. L.; Yun, W. *J. Am. Chem. Soc*. **1994**, *116*, 5523.
20. Frisch, M. J.; Trucks, G. W.; Schlegel, H. B.; Gill, P. M. W.; Johnson, B. G.; Robb, M. A.; Cheeseman, J. R.; Keith, T.; Petersson, G. A.; Montgomery, J. A.; Raghavachari, K.; Al-Laham, M. A.; Zakrzewski, V. G.; Ortiz, J. V.; Foresman, J. B.; Cioslowski, J.; Stefanov, B. B.; Nanayakkara, A.; Challacombe, M.; Peng, C. Y.; Ayala, P. Y.; Chen, W.; Wong, M. W.; Andres, J. L.; Replogle, E. S.; Gomperts, R.; Martin, R. L.; Fox, D. J.; Binkley, J. S.; Defrees, D. J.; Baker, J.; Stewart, J. P.; Head-Gordon, M.; Gonzalez, C.; Pople, J. A. Gaussian 94, Revision E.2; Gaussian, Inc., Pittsburgh PA, 1995.
21. Becke, A. D. *J. Chem. Phys*. **1993**, *98*, 5648.
22. Mulliken, R. S. *J. Chem. Phys*. **1955**, *23*, 1833.
23. Hehre, W. J.; Radom, L.; Schleyer, R. v. R.; Pople, J. A. *Ab Initio Molecular Orbital Theory*; Wiley-Interscience: New York, 1986; pp 25–29.
24. Breneman, C. M.; Wiberg, K. B. *J. Comp. Chem*. **1990**, *11*, 361.
25. Eis, P. S.; Smith, J. A.; Rydzewski, J. M.; Case, D. A.; Boger, D. L.; Chazin, W. J. *J. Mol. Biol*. **1997**, *272*, 237.
26. Eis, P. S.; Smith, J. A.; Case, D. A.; Chazin, W. J. Protein Data Bank structure 1DSA.
27. Colored graphical depictions of the HOMO and LUMO orbitals for the neutral *N*-Ac-DSA can be obtained from the authors.
28. Stowasser, R.; Hoffman, R. *J. Am. Chem. Soc*. **1999**, *121*, 3414.